Dynamics of electrically driven sub-nanosecond switching in Vanadium dioxide

Matthew Jerry[1], Nikhil Shukla[1], Hanjong Paik[2], Darrell G. Schlom[2], and Suman Datta[1]
[1]Electrical Engineering, University of Notre Dame, Notre Dame, USA
[2]Materials Science and Engineering, Cornell University, Ithaca, USA
Email: mjerry@nd.edu Phone: 413-230-0144

Abstract — **The switching dynamics of electrically driven insulator-to-metal transition (IMT) and metal-to-insulator transition (MIT) in vanadium dioxide are investigated. The transient response of time domain measurements are modeled using a domain based 2-D heterogeneous resistive network, taking into account local electronic potential and local Joule heating. It reveals, the switching time is dominated by a spatially non-uniform percolation of the metallic phase during the IMT driven by electro-thermal forces. We demonstrate an IMT switching time of 793ps in scaled VO_2 devices and project IMT and MIT switching speed for scaled devices.**

I. INTRODUCTION

Vanadium dioxide (VO_2) exhibits an insulator-to-metal transition (IMT) at 340K in bulk, characterized by up to five orders of magnitude change in resistivity [1]. The ability to electrically induce a phase transition implies the opportunity of VO_2 in abrupt electronic switches as selectors for three dimensional cross-point memories, steep slope Phase-FETs (Fig. 1(b)), and coupled oscillator network [2], [3]. In this work, we explore the fundamental dynamics of the reversible phase transition in two terminal VO_2 devices as a function of dimensions, with the goal to optimize its high speed switching capability during both IMT and MIT.

II. CHARACTERIZATION AND RESULTS

Fig. 2 illustrates the effect of varying pulse amplitudes (V_{IN}) and pulse widths (PW) on the speed of the IMT (τ_{IMT}) and metal-to-insulator transition (MIT) (τ_{MIT}). Transient measurements show that, for small V_{IN}, the IMT occurs in sets of multiple abrupt events (τ_{IMT_1}). This is attributed to a spatially non-uniform transition characterized by regions of phase coexistence experimentally measured using spatially resolved microwave impedance spectroscopy [4]. We have developed a 2-D heterogeneous resistive network (Fig 3(a)) to explain the empirical results quantitatively. The VO_2 device is described as a rectangular grid of domains (n=45;m=84) each independently capable of undergoing IMT or MIT. Domains are allowed to undergo transition based on the local potential drop, ΔV, across it and local temperature. The probability of a potential dependent transition is calculated from equations (1)-(3) [4].

$$\Delta V = ((V_1 - V_3)^2 + (V_2 - V_4)^2)^{1/2} \tag{1}$$

$$P_{IMT} = e^{-(E_B - q\Delta V)/kT} \tag{2}$$

$$P_{MIT} = e^{-(E_B - E_c)/kT} \tag{3}$$

The probability of a temperature initiated transition is calculated based on the power generated due to the local current flow from equation (4) [5].

$$\frac{\partial T_{n,m}}{\partial t} c = P_{n,m} - \kappa\left(4T_{n,m} - \sum_i^{1st\ neighbors} T_i\right) + h_d\left(T_{ext} - T_{n,m}\right) \tag{4}$$

The measured and simulated switching results, for low and high V_{IN}, are compared in Figs. 3(b)-(c) & Figs. 4(a)-(b). The model captures the discontinuous switching observed experimentally for V_{IN}=1.4V and captures the faster single abrupt switching for V_{IN}=2.1V. The respective domain state and temperature maps of the channel are shown in Figs. 3(d) & 4(c). Fig. 5 shows the device scaling trends for τ_{IMT}. The reduction in device area reduces the total area over which the IMT must propagate and improves the switching performance. Fig. 6 shows the device scaling normalized at V_{IN}=2.2V. 793 picosecond switching is observed in a L_{VO2}=100nm & W_{VO2}=300nm device (Fig. 7). The role of joule heating on τ_{MIT} is highlighted in Fig. 8, where increasing V_{IN} and PW causes increased and prolonged joule heating raising the local domain temperatures and prolonging τ_{MIT}. Due to the conflicting dependence of τ_{IMT} and τ_{MIT} on V_{IN} an optimal operating point exists for a complete cycle of switching. The trade off is shown in Fig. 9 where low V_{IN} requires longer pulse widths due to the longer τ_{IMT} and higher voltages cause excessive power generation in the channel. Using the 2-D heterogeneous resistive network we capture and predict the scaling trends for the total switching cycle as the device dimensions are reduced (Fig. 10).

III. CONCLUSION

In summary, we experimentally demonstrate sub-nanosecond (793ps) switching in VO_2 through dimensional scaling. A 2-D model quantitatively explains the electro-thermal IMT in the high and low voltage regimes, while the MIT is found to be limited by joule heating. We show scaling L_{VO2}, W_{VO2}, input voltage pulse width and amplitude, minimizes the area over which the IMT must propagate and can limit joule heating improving both τ_{IMT} and τ_{MIT}. This demonstrates a design space and pathway toward realizing high-speed abrupt switches and oscillatory devices in VO_2.

ACKNOWLEDGEMENTS

This work was supported in part by INTEL customized SRC and by the Center for Low Energy Systems Technology (LEAST), one of the six SRC STARnet Centers, sponsored by MARCO and DARPA.

References:
[1] L. A. Ladd *et al.*, Solid State Commun. 7 425 (1969)
[2] N. Shukla *et al.*, Nat. Commun., vol. 6, p. 7812, 2015.
[3] N.Shukla *et al.*, IEDM 2014, pp. 28.7.1-28.7.4
[4] H. Madan *et al.*, ACS Nano, vol. 9, no. 2, pp. 2009-17, 2015.
[5] P. Stoliar *et al.*, Phys. Rev. B, vol. 90, no. 4, p. 045146, 2014.

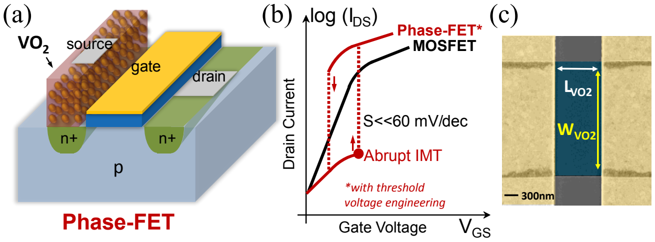

Fig. 1. (a) Phase-FET schematic showing integrated structure. (b) Transfer characteristics comparing MOSFET and Phase-FET. (c) SEM image of a two-terminal VO_2 device used to characterize VO_2 switching speed.

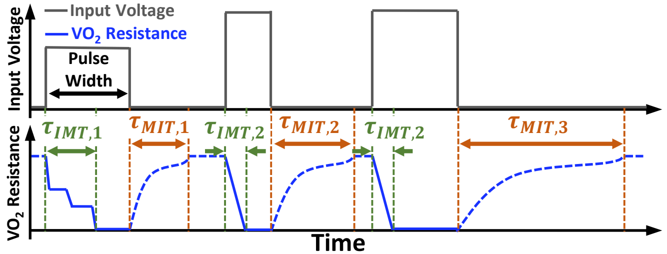

Fig. 2. Schematic representation of the effects of input voltage pulse on τ_{IMT} and τ_{MIT}. Higher V_{IN} results in increased local potential drops and joule heating across the nano-domain structure enhancing the speed of the IMT transition.

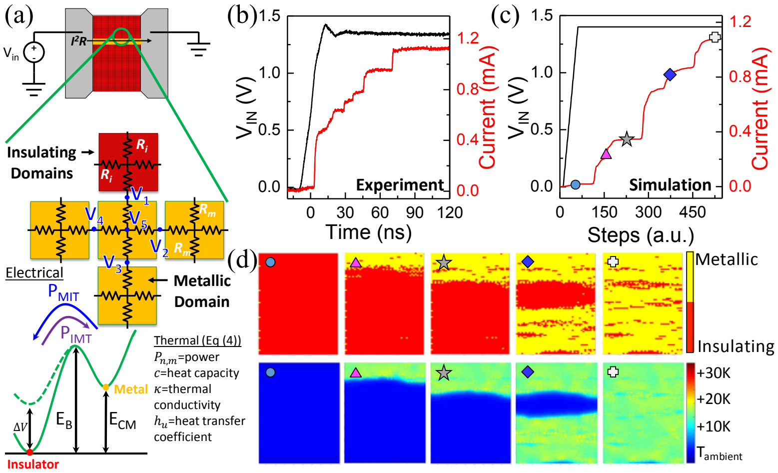

Fig. 3. (a) 2-D heterogeneous resistive network used to model the filamentary nature of conduction in VO_2. (b)(c) Measured and simulated switching transient at V_{IN}=1.4V. (d) Corresponding nanoscale channel domain structure and temperature during switching.

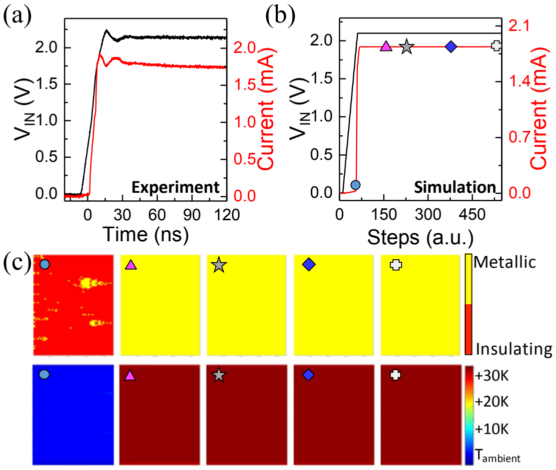

Fig. 4. (a) Measured waveform for V_{IN}=2.1V. (b) Simulated switching for V_{IN}=2.1V and (d) corresponding channel domain structure and locally computed temperature.

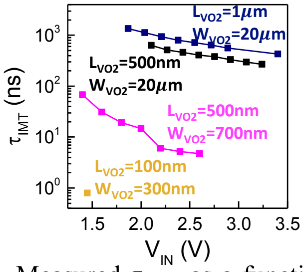

Fig. 5. Measured τ_{IMT} as a function of input bias for varying device sizes; lengths from 1µm - 100nm and widths from 20µm - 300nm.

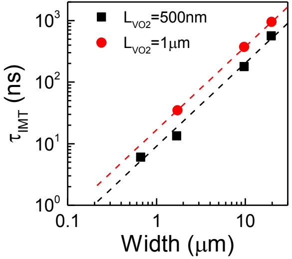

Fig. 6. τ_{IMT} scaling trends for W_{VO2} and L_{VO2} normalized to V_{IN}=2.2V. Red and black broken lines serve as a guide to the eyes.

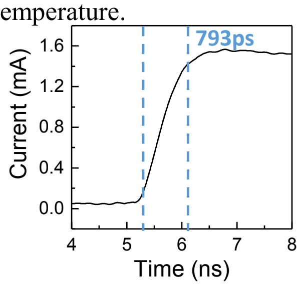

Fig. 7. Sub-nanosecond switching (793ps) for device size: L_{VO2}= 100nm, W_{VO2}=300nm at V_{IN}=1.45V.

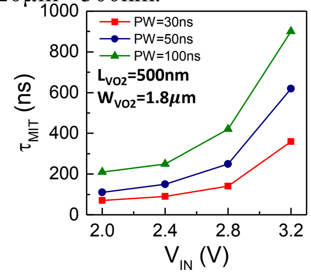

Fig. 8. τ_{MIT} as a function of input bias. Increasing V_{IN} or PW causes greater joule heating within the VO_2 device lengthening the thermal dissipation time.

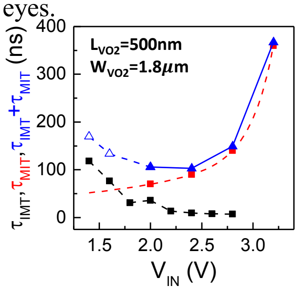

Fig. 9. Measured $\tau_{IMT} + \tau_{MIT}$ as a function of V_{IN} (PW=30ns). An optimal operating point exists due to differing dependence of τ_{IMT} and τ_{MIT} on V_{IN}.

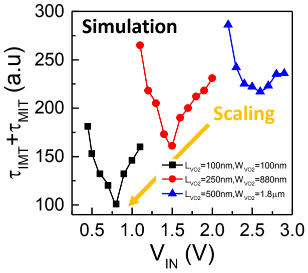

Fig. 10. Simulated scaling trends for $\tau_{IMT} + \tau_{MIT}$ highlighting the benefit coming from area, pulse width, and switching voltage reduction.